THE JOURNAL OF BIOLOGICAL CHEMISTRY VOL. 291, NO. 49, pp. 25608–25616, December 2, 2016

Potent and Selective Peptide-based Inhibition of the G Protein $G\alpha_q$*

Received for publication, May 27, 2016, and in revised form, October 13, 2016 Published, JBC Papers in Press, October 14, 2016, DOI 10.1074/jbc.M116.740407

Thomas H. Charpentier[‡§1], **Gary L. Waldo**[‡], **Emily G. Lowery-Gionta**[‡], **Krzysztof Krajewski**[¶‖], **Brian D. Strahl**[¶‖], **Thomas L. Kash**[‡], **T. Kendall Harden**[‡], **and John Sondek**[‡§¶2]

From the Departments of [‡]*Pharmacology and* [¶]*Biochemistry and Biophysics,* [‖]*High-Throughput Peptide Synthesis and Array Facility, and* [§]*Lineberger Comprehensive Cancer Center, University of North Carolina School of Medicine, Chapel Hill, North Carolina 27599*

Edited by Norma Allewell

In contrast to G protein-coupled receptors, for which chemical and peptidic inhibitors have been extensively explored, few compounds are available that directly modulate heterotrimeric G proteins. Active $G\alpha_q$ binds its two major classes of effectors, the phospholipase C (PLC)-β isozymes and Rho guanine nucleotide exchange factors (RhoGEFs) related to Trio, in a strikingly similar fashion: a continuous helix-turn-helix of the effectors engages $G\alpha_q$ within its canonical binding site consisting of a groove formed between switch II and helix α3. This information was exploited to synthesize peptides that bound active $G\alpha_q$ *in vitro* with affinities similar to full-length effectors and directly competed with effectors for engagement of $G\alpha_q$. A representative peptide was specific for active $G\alpha_q$ because it did not bind inactive $G\alpha_q$ or other classes of active $G\alpha$ subunits and did not inhibit the activation of PLC-β3 by $G\beta_1\gamma_2$. In contrast, the peptide robustly prevented activation of PLC-β3 or p63RhoGEF by $G\alpha_q$; it also prevented G protein-coupled receptor-promoted neuronal depolarization downstream of $G\alpha_q$ in the mouse prefrontal cortex. Moreover, a genetically encoded form of this peptide flanked by fluorescent proteins inhibited $G\alpha_q$-dependent activation of PLC-β3 at least as effectively as a dominant-negative form of full-length PLC-β3. These attributes suggest that related, cell-penetrating peptides should effectively inhibit active $G\alpha_q$ in cells and that these and genetically encoded sequences may find application as molecular probes, drug leads, and biosensors to monitor the spatiotemporal activation of $G\alpha_q$ in cells.

G protein-coupled receptors (GPCRs)[3] are the largest family of cell surface receptors in eukaryotes and regulate essentially all physiological processes (1–4). Scores of neurotransmitters, hormones, and other extracellular signaling molecules promote conserved conformational changes in GPCRs that favor interaction with heterotrimeric G proteins ($G\alpha\beta\gamma$) on the inner leaflet of the plasma membrane. The subsequent exchange of GTP for GDP alters three switch regions within $G\alpha$ subunits to promote dissociation from $G\beta\gamma$ (5, 6). These activated subunits then directly stimulate downstream effectors, leading to propagation and amplification of signaling pathways (7, 8).

Signaling cascades downstream of several hundred different GPCR are activated by the cognate agonist of these receptors. Many of these GPCRs, particularly those activated by neurotransmitters, also have been targeted by receptor subtype-selective agonists and antagonists. Indeed, up to a quarter of current top-prescribed, Food and Drug Administration-approved drugs take advantage of GPCR-selective targeting. In contrast, few molecular probes are available for dissection of the downstream signaling cascades emanating from these GPCRs. Most notably, bacterially derived cholera and pertussis toxins contributed enormously to the initial identification of $G\alpha_s$ and $G\alpha_i$ and were subsequently applied to differentiate $G\alpha_s$- and $G\alpha_i$-mediated signaling pathways (9). However, only a few small molecules have been identified that target $G\alpha$ subunits, and reliable pharmacological agents that selectively inhibit these signaling proteins are not generally available (10). For example, BIM-46174 and BIM-46187 apparently interact with most $G\alpha$ subunits (11, 12), and some selectivity for $G\alpha_q$ has been reported for BIM-46187 (13). In contrast, YM-254890 (14), and related natural products such as FR900359 (15, 16), specifically inhibit $G\alpha$ subunits of the G_q family (17, 18), and a crystal structure of a G protein heterotrimer bound to YM-254890 illustrates that this molecule prevents GDP release and heterotrimer dissociation (19). Unfortunately, synthesis of cyclic depsipeptides is difficult, and YM-254890 remains unavailable from commercial sources. The mechanism of this molecule also precludes inhibition against $G\alpha$ subunits in the GTP-bound state; for example, on mutant proteins that are constitutively active because of loss of GTPase function.

Linear peptides also have been identified that selectively target $G\alpha$ subunits (20). For example, the G protein regulatory

* This work was supported by National Institutes of Health Grants R01-GM057391 (to J. S. and T. K. H), R01-AA019454 and U01-AA020911 (to T. L. K.), and AA022549 (to E. G. L. G.) and by a Melanoma Research Foundation grant (to J. S.). The authors declare that they have no conflicts of interest with the contents of this article. The content is solely the responsibility of the authors and does not necessarily represent the official views of the National Institutes of Health.

[1] Supported by the American Cancer Society (PF-12-153-01-DMC).

[2] To whom correspondence should be addressed: Depts. of Pharmacology, and Biochemistry and Biophysics and Lineberger Comprehensive Cancer Center, University of North Carolina School of Medicine, 120 Mason Farm Rd., Chapel Hill, NC 27599. Tel.: 919-966-7530; E-mail: sondek@med.unc.edu.

[3] The abbreviations used are: GPCR, G protein-coupled receptor; PLC, phospholipase C; HTH, helix-turn-helix; Nle, norleucine; PFC, prefrontal cortex; CCh, carbachol; GEF, guanine nucleotide exchange factor; TAMRA, carboxytetramethylrhodamine; DOI, 2,5-dimethoxy-4-iodoamphetamine; PIP_2, phosphatidylinositol 4,5-bisphosphate.

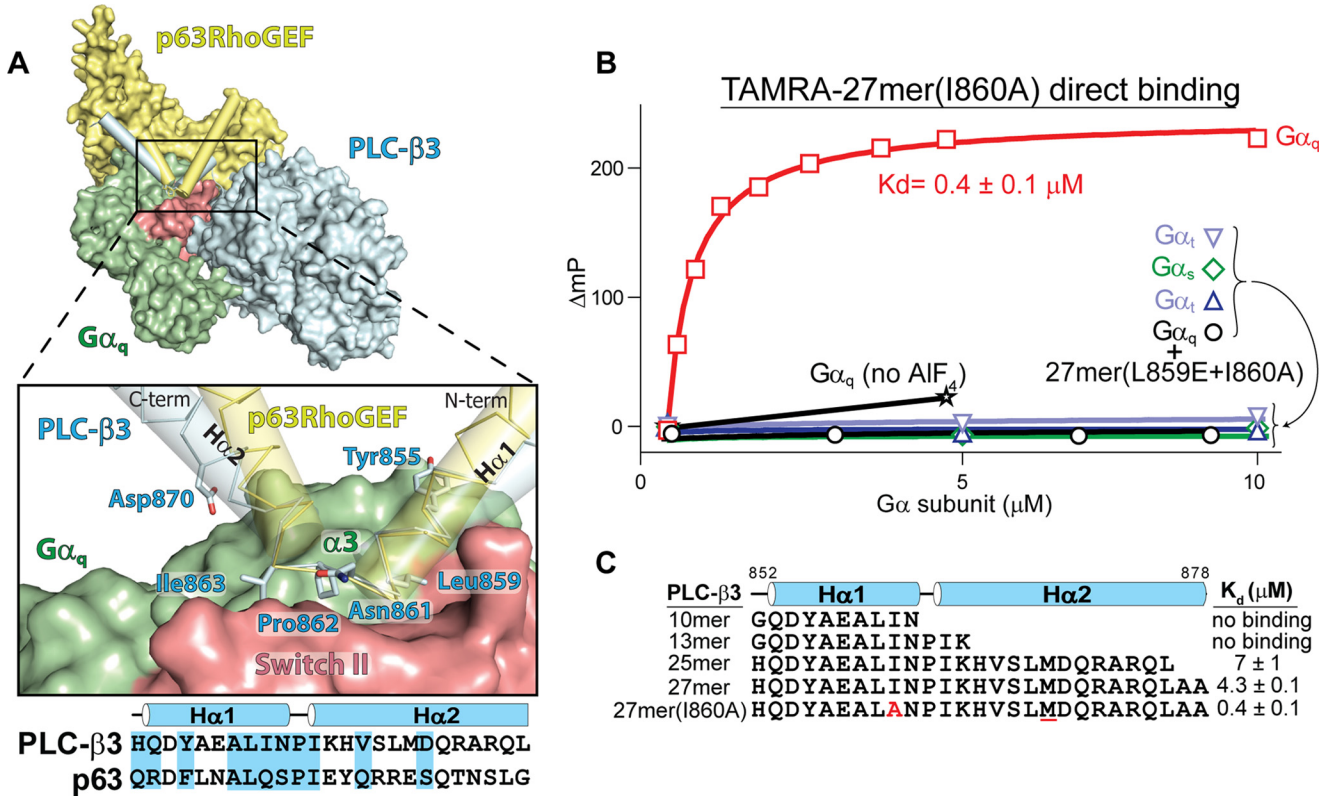

FIGURE 1. **Gα$_q$ uses a conserved mechanism to engage effectors.** *A*, a helix-turn-helix (Hα1/Hα2, *cylinders*) in either PLC-β3 (*blue*) or p63RhoGEF (*yellow*) engages a shallow groove on activated Gα$_q$ (*green* with switch regions in *red*) between switch II and α3. The structures of Gα$_q$ bound to either PLC-β3 (PDB code 3OHM) (30) or p63RhoGEF (PDB code 2RGN) (31) were superimposed using Gα$_q$. For clarity, only a single Gα$_q$ is shown. The *expanded region* highlights residues in PLC-β3 that directly contact Gα$_q$; contacts *boxed* in the corresponding sequence alignment. *C-term*, C terminus; *N-term*, N terminus. *B* and *C*, peptides derived from the helix-turn-helix of PLC-β3 selectively bind active Gα$_q$. *B*, fluorescence polarization (Δ*mP*, change in millipolarization) was used to measure the binding of the indicated Gα subunits to either a TAMRA-labeled peptide (27-mer(I860A)) derived from the helix-turn-helix of PLC-β3 or the equivalent peptide also containing L859E (27-mer(L859E+I860A)). All Gα subunits were activated with aluminum fluoride except where indicated (no *AlF$_4$*). *C*, the above assay was used to measure affinities of active Gα$_q$ for the TAMRA-labeled peptides listed. Substitutions include I860A (*red*) and M869Nle (*underlined in red*).

(GPR or GoLoco) motif of proteins preferentially binds GDP-bound Gα$_i$ subunits with relatively high affinity to decrease spontaneous nucleotide exchange (21). Small peptides based on this motif were applied to inhibit D2 dopamine receptor-stimulated potassium channel currents (22). Phage display in combination with Gα$_{i1}$ was also used to generate peptides that specifically bind Gα subunits dependent on the state of bound nucleotide (23–25). One of these peptides preferentially binds active Gα$_i$ and Gα$_t$ and was shown to inhibit the capacity of Gα$_{i1}$ to be inactivated by RGS12 and to reduce activation of cGMP phosphodiesterase by Gα$_t$ in membrane preparations.

A molecular understanding of the binding of Gα subunits with their downstream effectors potentially informs the development of peptides to pharmacologically antagonize functional interaction of these signaling cohorts. For example, rearrangement of the switch regions of Gα subunits creates a hydrophobic cleft between switch 2 and α helix 3 that is a major site of interaction with effectors (26) and potentially exists as a site for drug targeting. The best understood Gα/effector interaction is between Gα$_q$ and its effectors, the phospholipase C-β (PLC-β) isozymes and the related Dbl family proteins p63RhoGEF, Trio, and kalirin (27–29). These effectors engage the hydrophobic cleft of Gα$_q$ using almost identical sets of interactions derived from a helix-turn-helix (HTH) substructure (Fig. 1) that is induced in the effectors upon engagement with Gα$_q$. The HTH of PLC-β3 and p63RhoGEF forms the major interface with Gα$_q$ in crystal structures of these complexes, whereas secondary interactions orient the complexes at membranes for efficient effector activation (30, 31).

Here we show that linear peptides based on the HTH of PLC-β3 specifically bind activated Gα$_q$ to prevent engagement and activation of downstream effectors by Gα$_q$. These peptides have no appreciable affinity for either GDP-bound Gα$_q$ or for activated forms of other Gα subunits and should be useful reagents for interdicting signaling cascades controlled by Gα$_q$. Indeed, we show that microinjection of HTH-based peptides into mouse neurons of the prefrontal cortex prevents depolarization downstream of muscarinic cholinergic receptor-dependent activation of Gα$_q$.

Results

Canonical Effector Interactions with Gα$_q$ Drive Complex Formation—Recent structures of activated Gα$_q$ bound to either PLC-β3 (30) or p63RhoGEF (31) highlight an essentially identical mechanism of effector engagement. In both cases, an HTH of the effector occupies the canonical effector-binding site of Gα$_q$ composed of a shallow groove between the α3 helix and switch II (Fig. 1*A*). The HTH is presumed to provide the majority of favorable interactions promoting complex formation and buries ~810 Å^2 of Gα$_q$ (5% of the accessible surface) to produce

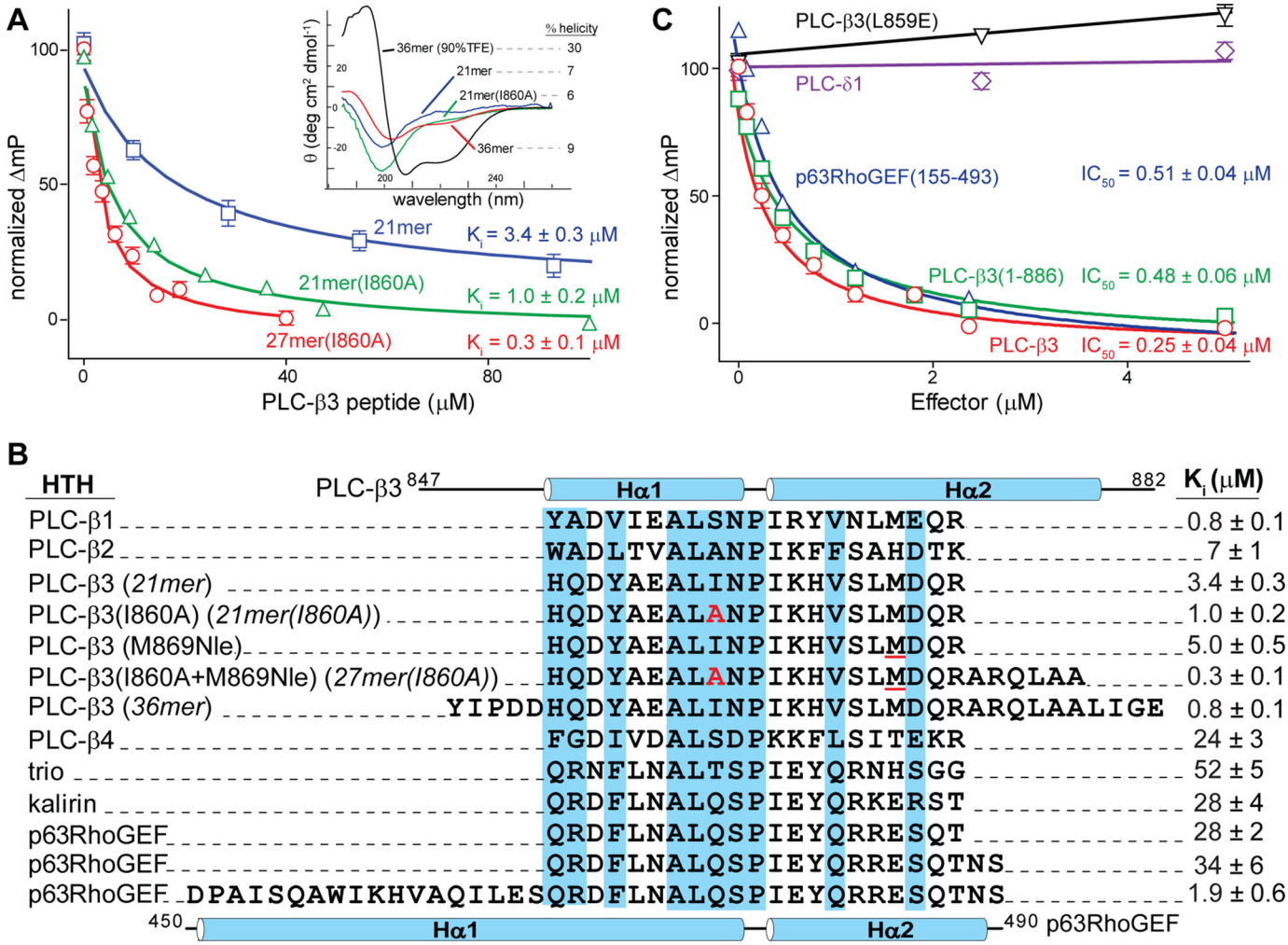

FIGURE 2. **Competition assay to measure affinities of peptides and effectors for Gα$_q$.** *A* and *B*, individual unlabeled peptides were titrated into a solution of Gα$_q$ bound to TAMRA-27-mer(I860A), and fluorescence polarization was measured. K_i values were calculated using an equation to convert IC_{50} to K_i values in fluorescence-based competition assays (38). The sequence alignment is annotated as in Fig. 1. *Inset*, circular dichroism spectra for select peptides. Substitutions include I860A (*red*) and M869Nle (*underlined in red*). *C*, competition assay used to measure affinities of the indicated effectors for Gα$_q$ activated with aluminum fluoride.

the largest contiguous interface between proteins in these structures. Deletion of the HTH of PLC-β3 (30) or p63RhoGEF (29) abrogates interaction with Gα$_q$; conversely, grafting the HTH of PLC-β3 onto PLC-δ1 engenders complex formation with Gα$_q$ (30).

To more accurately quantify interactions between activated Gα$_q$ and HTH peptides, changes in fluorescence polarization were measured for a set of TAMRA-labeled peptides spanning the HTH of PLC-β3 and titrated with various Gα subunits (Fig. 1, *B* and *C*). A 27-residue peptide (27mer(I860A)), derived from the complete HTH of PLC-β3, bound to activated Gα$_q$ with high affinity (K_d ~400 nM), and complex formation was dependent upon activation because little change in fluorescence occurred in the absence of aluminum fluoride (Fig. 1*B*). This interaction was also specific for Gα$_q$ because activation of other Gα subunits (Gα$_{i1}$, Gα$_t$, and Gα$_s$) did not result in binding to the HTH-based peptide. A residue on the HTH that is a major contributor to this interaction is leucine at position 859 of PLC-β3, and mutating this residue to glutamic acid abolished binding of the TAMRA-labeled 27-mer(I860A) (Fig. 1*B*).

The 27-mer(I860A) peptide contains two substitutions relative to the wild-type sequence: the oxidation-prone methionine was replaced with isosteric L-norleucine, and isoleucine at position 860 of full-length PLC-β3 was replaced with alanine (Fig. 1*C*). This second substitution (I860A) was shown previously to increase the phospholipase activity of PLC-β3 in response to Gα$_q$ (30) and was assumed to increase the affinity of the complex. Indeed, the substitutions contributed to an approximate 10-fold increase in affinity for activated Gα$_q$ compared with the equivalent peptide (27-mer) without substitutions (Fig. 1C). Truncation of the 27-mer by removal of two alanines at its C terminus (25-mer) led to a minor reduction (< 2-fold) in affinity for Gα$_q$. In contrast, shorter peptides lacking most (13-mer) or all (10-mer) of the C-terminal helix of the HTH did not bind activated Gα$_q$ with measurable affinity.

The robust increase in fluorescence polarization produced by the complex of TAMRA-27-mer(I860A) with active Gα$_q$ was used in a series of competition binding experiments to assess the relative affinities of unlabeled peptides for active Gα$_q$ (Fig. 2). The capacity of unlabeled 27-mer(I860A) to interact with

Gα$_q$ was quantified by titrating this peptide into a solution containing 0.4 μM TAMRA-labeled peptide and active Gα$_q$. The resulting decrease in fluorescence polarization was quantified, and a K_i (~0.3 μM) for unlabeled 27-mer(I860A) was calculated as described under "Experimental Procedures" (Fig. 2*A*). This K_i was essentially identical to the K_d (~0.4 μM) determined for direct binding of the TAMRA-labeled 27-mer(I860A) to active Gα$_q$. Thus, the presence of the TAMRA moiety does not appreciably affect Gα$_q$-HTH complex formation.

A shorter, unlabeled peptide (21-mer(I860A)) that retained all PLC-β3 residues that contact Gα$_q$ in the complex (30) also effectively inhibited (K_i ~1 μM) the binding of TAMRA-27-mer(I860A). Binding was also more favorable with this peptide than with the equivalent 21-mer without substitution (Fig. 2*A*), which again supports the idea that the I860A substitution enhances complex formation. The ~3-fold decrease in inhibitory activity of 21-mer(I860A) relative to 27-mer(I860A) is consistent with direct binding measurements that showed a slight decrease in the affinity of the TAMRA-labeled 25-mer relative to the equivalent 27-mer. This trend also held in comparisons of the activity of unlabeled, unsubstituted 21-mer of PLC-β3 (K_i ~3 μM) with that of the related 36-mer (K_i ~1 μM) (Fig. 2*B*).

The reason(s) why the shorter peptides exhibit a small but consistent decrease in affinity for Gα$_q$ relative to the longer forms is unclear. One possibility is that loss of residues either proximal to or contained within the helices of the HTH motif destabilizes the secondary structure needed for complex formation with Gα$_q$. This destabilization is likely to manifest only after formation of the complex because, irrespective of their length, the isolated peptides exhibit minimal helical content based on circular dichroism spectroscopy (Fig. 2*A*, *inset*). If true, this destabilization would result in higher off rates for the shorter peptides in complex with Gα$_q$.

Peptides (21-mers) corresponding to the HTH portions of the four PLC-β isozymes exhibited a 25-fold range of inhibitory activities (Fig. 2*B*). Interestingly, these relative activities correlate with the general capacity of Gα$_q$ to activate these isozymes (PLC-β1 ~ β3 > β2 > β4) (32, 33), suggesting that Gα$_q$-mediated activation of PLC-β isozymes is principally a function of complex formation driven by the affinity of Gα$_q$ for the HTH region. Equivalent 21-mers from p63RhoGEF and the related GEFs Trio and kalirin exhibited K_i values in the range of ~25–50 μM, which is similar to the inhibitory activity observed with the HTH of PLC-β4. Relative to the equivalent portion in PLC-β3, the first helix of the HTH is substantially longer in the structure of p63RhoGEF bound to Gα$_q$. Consistent with previous results, extension of a peptide of p63RhoGEF to include the entire first helix increased inhibitory activity ~15-fold relative to the cognate 21-mer (Fig. 2*B*).

The competition assay was also useful for quantifying relative affinities of active Gα$_q$ and full-length effectors. For example, full-length PLC-β3 prevented engagement of active Gα$_q$ by TAMRA-27-mer(I860A) with an IC_{50} of ~250 nM (Fig. 2*C*). This inhibitory activity was ~3-fold greater than that of the 36-mer of PLC-β3, indicating that most of the energetically favorable interactions with Gα$_q$ reside within the HTH of PLC-β3.

The C-terminal domain of PLC-β isozymes is required for phospholipase activation by Gα$_q$ at membranes; however, measurements of the contribution of the C-terminal domain to binding to Gα$_q$ have ranged from essentially no effect (30, 34) to promoting complex formation by at least 2 orders of magnitude (35). Related to this discrepancy, a truncated form (residues 1–886) of PLC-β3, which retains the HTH but lacks the entire C-terminal domain, competed for complex formation (Fig. 2*C*) with an inhibitory activity within 2-fold of that observed with full-length PLC-β3. This result is consistent with previous affinity measurements using surface plasmon resonance assays that indicated that the C-terminal domain of PLC-β3 is responsible for less than a 2-fold increase in affinity for Gα$_q$ relative to PLC-β3(1–886) (30). Conversely, a single substitution (L859E) within the HTH of full-length PLC-β3 that was shown previously to prevent activation of PLC-β3 by Gα$_q$ (30) completely abrogated the capacity of full-length PLC-β3 to compete with the TAMRA-labeled peptide for engagement of Gα$_q$ (Fig. 2*C*). In addition, PLC-δ1 was not responsive to Gα$_q$ and was incapable of competing with TAMRA-27-mer(I860A) (Fig. 2*C*).

Finally, a large fragment (residues 155–493) of p63RhoGEF that includes its HTH effectively competed (IC_{50} ~500 nM) with TAMRA-27-mer(I860A) for engagement of Gα$_q$ (Fig. 2*C*). A relative K_i of 1.9 μM was observed for binding of the isolated HTH of p63RhoGEF to Gα$_q$, and, therefore, as was observed with PLC-β3, the majority of favorable interactions for complex formation with Gα$_q$ reside within the HTH of p63RhoGEF.

Inhibition of Gα$_q$-mediated Signaling in Vitro—Because peptides derived from the HTH of PLC-β3 effectively compete with effectors for engagement of Gα$_q$, these peptides should also prevent the Gα$_q$-dependent activation of these effectors. As illustrated in Fig. 3*A*, TAMRA-27-mer(I860A) indeed efficiently blocked Gα$_q$-mediated activation of purified PLC-β3 in reconstituted lipid vesicles. Inhibition was dependent on the concentration of peptide as well as Gα$_q$. A 5-fold increase in the concentration of Gα$_q$ required a corresponding increase in peptide concentration to achieve equivalent inhibition of phospholipase activity with no change in the shape of the concentration-effect curve. These results are strongly indicative of direct competitive inhibition by the peptide to prevent functional engagement of PLC-β3 by Gα$_q$, which is expected if both peptide and effector share a common interface on Gα$_q$.

Although the presence of TAMRA had no apparent effect on HTH-Gα$_q$ binding in solution, removal of the TAMRA moiety from the peptide reduced inhibition of phospholipase activity by ~5-fold (IC_{50} ~200 nM) (Fig. 3*B*), suggesting that the fluorescent group has nonspecific affinity for membranes. This idea is also supported by the observation that TAMRA-27-mer(L859E+I860A) did not inhibit Gα$_q$-mediated activation of PLC-β3 under identical conditions and that, therefore, TAMRA *per se* does not intrinsically inhibit activation. TAMRA-27-mer(I860A)-mediated inhibition of phospholipase activity was specific for Gα$_q$ because the peptide did not inhibit the equivalent activation of PLC-β3 by Gβ$_1$γ$_2$ (Fig. 3*C*). Indeed, under conditions of synergistic activation of PLC-β3 by both Gβ$_1$γ$_2$ and Gα$_q$, only the Gβγ-mediated component of activation appeared to be preserved in the presence of TAMRA-27-mer(I860A).

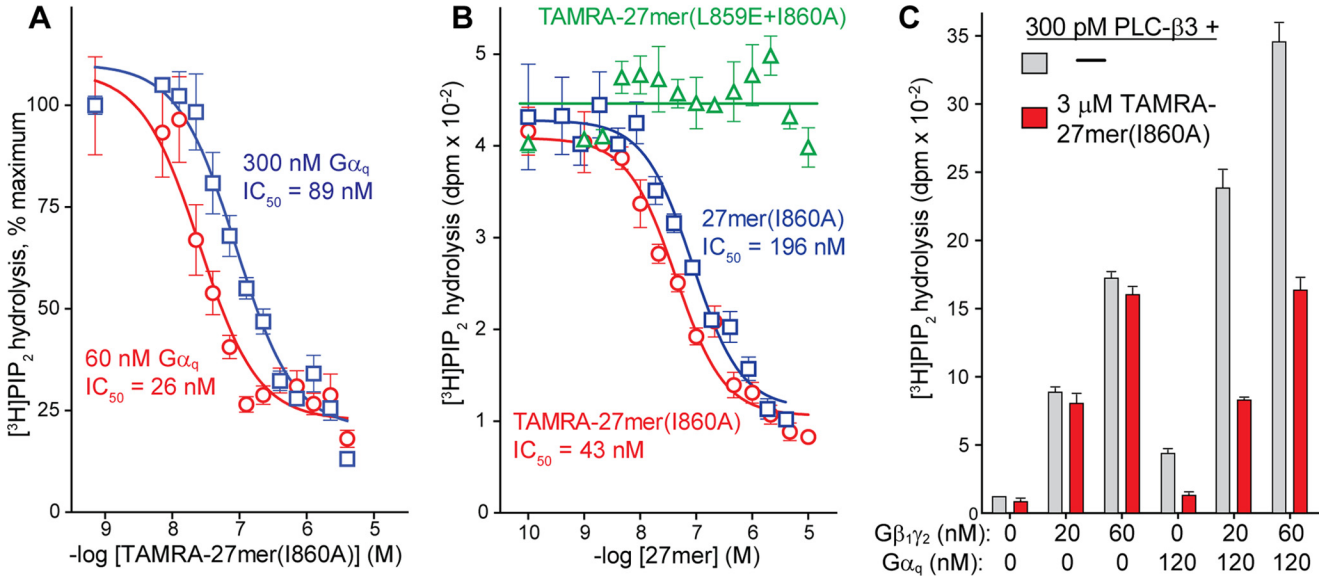

FIGURE 3. **27-mer(I860A) inhibits active Gα$_q$ in lipid vesicles.** *A* and *B*, lipid vesicles containing [^{3}H]PIP$_2$ were reconstituted with PLC-β3 and Gα$_q$ prior to measuring hydrolysis of PIP$_2$ in the presence of increasing concentrations of the indicated peptides. 120 nM Gα$_q$ was used in *B*. *C*, TAMRA-27-mer(I860A) did not inhibit the capacity of Gβ$_1$γ$_2$ to activate PLC-β3 in lipid vesicles but prevented synergy with Gα$_q$.

Because the canonical effector-binding surface of Gα$_q$ is required for activation of both PLC isozymes and RhoGEFs, the capacity of 27-mer(I860A) to prevent activation of p63RhoGEF by Gα$_q$ was examined. Fluorescent GDP was preloaded onto RhoA, and the capacity of Gα$_q$ to stimulate p63RhoGEF-promoted guanine nucleotide exchange by Rho was quantified in the presence of increasing concentrations of 27-mer(I860A) (Fig. 4). Activity was sharply reduced by 5 μM 27-mer(I860A) and completely inhibited by 12.5 μM 27-mer(I860A).

Inhibition of Gα$_q$-mediated Signaling in Cells—Given the robust capacity of synthetic versions of the HTH of PLC-β3 to inhibit effector activation by Gα$_q$ using purified components, versions of the 27-mer were expressed in HEK293 cells and assessed for their capacity to inhibit Gα$_q$-promoted signaling (Fig. 5).

Activity initially was assessed after expression of full-length versions of PLC-β3 rendered catalytically inactive by substitution (H332A) of the active site of the lipase (Fig. 5*A*). This approach presumed that heterologous expression of PLC-β3(H332A) would act in a dominant-negative fashion to prevent activation of endogenous PLC-β in response to agonist (DOI)-promoted stimulation of the co-expressed, Gα$_q$-coupled 5HT$_{2A}$ receptor. Indeed, expression of increasing amounts of PLC-β3(H332A) resulted in essentially complete inhibition of DOI-stimulated inositol phosphate accumulation. Importantly, this inhibitory activity was not observed (Fig. 5*A*) with PLC-β3(H332A+L859E), which introduces an additional substitution, L859E, shown previously to prevent complex formation of PLC-β3 with Gα$_q$.

Given the results with PLC-β3(H332A), we examined the inhibitory activity of a construct consisting of the sequence equivalent to 27-mer(I860A) flanked by two fluorescent proteins to foster intracellular stability. This construct also potently blocked 5HT$_{2A}$ receptor-dependent activation of phospholipase C in HEK293 cells (Fig. 5*B*), and introduction of L859E into this construct abrogated this inhibitory activity.

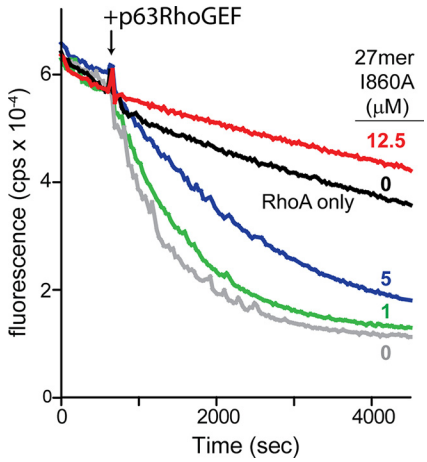

FIGURE 4. **Peptides derived from the helix-turn-helix of PLC-β3 inhibit the capacity of Gα$_q$ to activate p63RhoGEF.** RhoA (100 nM) preloaded with BODIPY-GDP was incubated with unlabeled GDP (2 μM), Gα$_q$ (100 nM), aluminum fluoride, and the indicated amounts of 27-mer(I860A) prior to measuring nucleotide exchange using fluorescence (*cps*, counts per second). p63RhoGEF (100 nM) was added as indicated. The trace marked *RhoA only* contains no Gα$_q$ or p63RhoGEF and indicates spontaneous nucleotide exchange.

Modification of the expression construct to direct posttranslation prenylation of the chimeric HTH peptide resulted in ~10-fold more efficient inhibitory activity of the 27-mer(I860A) sequence, and activity again was lost by introduction of the L859E mutation into the 27-mer(I860A) sequence (Fig. 5*C*).

An ultimate goal of this work is to develop peptidomimetic inhibitors of Gα$_q$-promoted signaling *in vivo*. Toward this goal, the capacity of these peptides to block neuronal depolarization was assessed (Fig. 6). Peptides were introduced into neuronal cells from slices of mouse prefrontal cortex via patch clamp prior to monitoring depolarization in response to muscarinic cholinergic receptor-promoted activation of a Gα$_q$ by the muscarinic agonist carbachol. Carbachol-stimulated current was similar to previously recorded activity (36) and was not affected

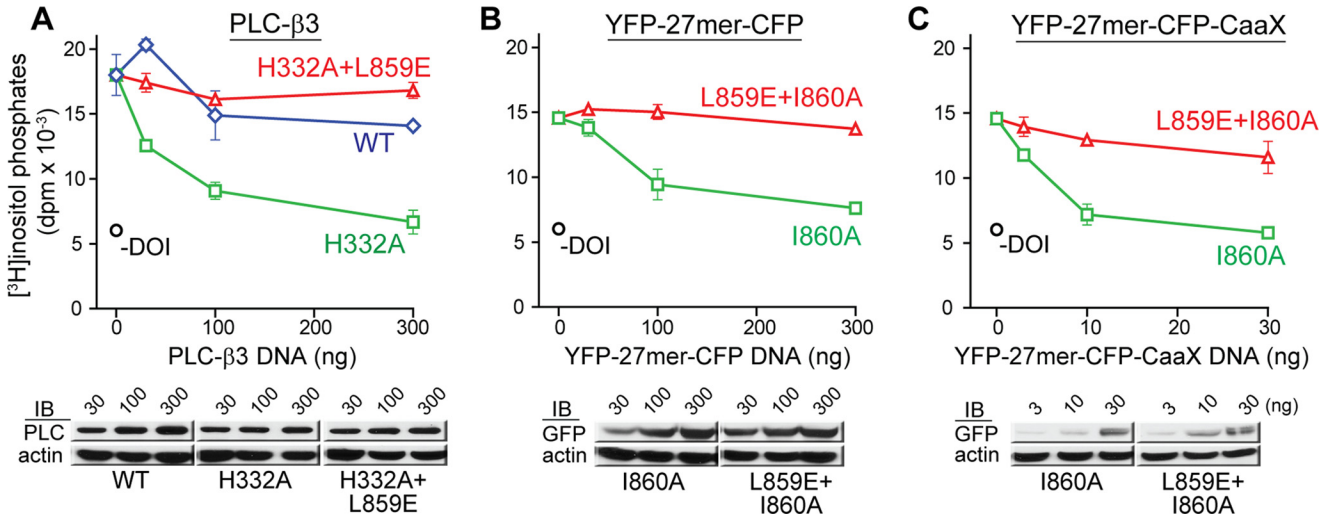

FIGURE 5. **Gα$_q$-dependent PLC-β3 activity in HEK293 cells is specifically inhibited by genetically encoded versions of the helix-turn-helix of PLC-β3.** *A–C*, HEK293 cells were co-transfected with expression vectors encoding the 5HT$_{2A}$ receptor (100 ng) and increasing amounts of PLC-β3 (*A*), YFP-27mer-CFP (*B*), or YFP-27mer-CFP-*CAAX* (*C*) variants prior to metabolic labeling of inositide pools, receptor activation with DOI (2 μM), and quantification of inositol phosphates. Protein expression and cellular totals (actin) were verified with Western blotting as shown. Cells without addition of agonist (−DOI) were also tested.

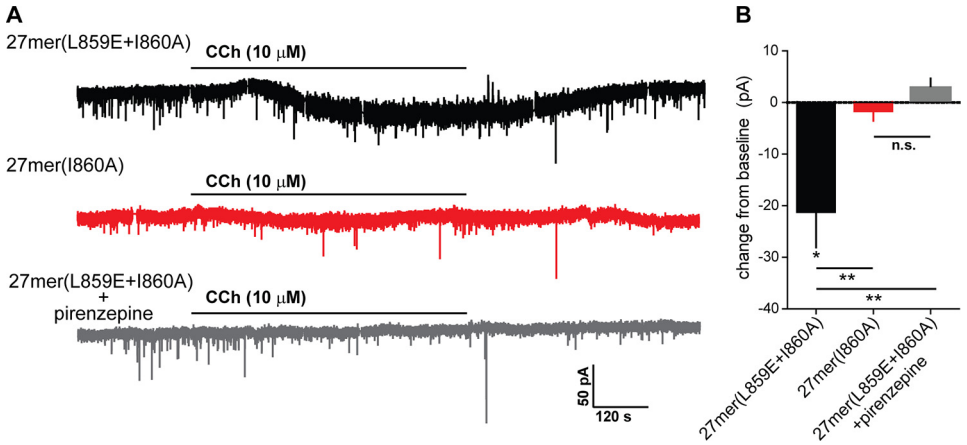

FIGURE 6. **27-mer(I860A) inhibits Gα$_q$-mediated neuronal depolarization in the prefrontal cortex of mice.** *A*, pretreatment of a representative prefrontal cortex neuron with 27-mer(L859E+I860A) had no effect on action potential firing in response to CCh (10 μM) (*top panel*). In contrast, depolarization was lost when 27-mer(I860A) was used (*center panel*) or the M1 receptor antagonist pirenzepine (2 μM) was applied with 27-mer(L859E+I860A) (*bottom panel*). *B*, the inward current induced by carbachol after indicated pretreatments. Sample sizes included six neurons for the active and inactive peptides and four neurons for the active peptide with agonist. *, $p < 0.05$ from baseline. **, $p < 0.05$ between the different experiments *n.s.*, not significant.

by injection of 10 μM 27-mer(L859E+I860A). In contrast, 10 μM 27-mer(I860A) completely blocked carbachol-stimulated depolarization, and this inhibition was similar to that observed after the simultaneous application of the muscarinic antagonist pirenzepine and 27-mer(L859E+I860A). Thus, a 27-mer based on the HTH of PLC-β3 blocks Gα$_q$-dependent signaling in a native neuronal system, and this inhibitory activity is lost after introduction of a mutation into the 27-mer known to result in loss of interaction of PLC-β3 with this G protein.

Discussion

The G$_q$-regulated effectors provide a striking illustration of converging evolution in disparate signaling proteins. We previously concluded that the HTH imparts most, if not all of, the binding energy for the complex of Gα$_q$ and PLC-β3, and this idea is confirmed here. Indeed, the equivalent region of p63RhoGEF and related GEFs appears also to embody most of the binding energy for complexation of these effectors with Gα$_q$.

Although the HTH of PLC-β3 is sufficient to recapitulate high-affinity interaction with active Gα$_q$, complex formation mediated by the HTH is insufficient to elevate phospholipase activity (30). This follows from the additional requirement of the ~250-residue carboxyl-terminal domain of the PLC, which, in combination with a membrane surface, is needed for activation. It remains unclear how these additional components impart activation, especially in light of the fact that the carboxyl-terminal domain likely provides no more than a 2-fold enhancement in affinity for Gα$_q$. However, one distinct possibility is that the carboxyl-terminal domain productively orients PLC-β3 at membranes for efficient interaction with Gα$_q$ and hydrolysis of membrane-resident phosphatidylinositol 4,5-bisphosphate. Other PLC-β isozymes would be activated similarly. Indeed, a similar membrane-induced steering of p63RhoGEF and related GEFs with

Gα$_q$ appears to be required for the efficient capacity of these GEFs to active RhoA (37).

Elucidation of the role of the HTH in Gα$_q$ binding to PLC-β isozymes together with the observation of dominant negative-like activity of a lipase-dead form of full-length PLC-β3 led us to investigate the cellular activity of a genetically encoded form of the HTH. Thus, a peptide optimized for binding to Gα$_q$ *in vitro* proved to markedly inhibit the stimulation of inositol lipid hydrolysis occurring downstream of the G$_q$-linked 5HT$_{2A}$ receptor. The increase in cellular potency of the peptide observed after introduction of a C*AAX* motif almost certainly occurs as a consequence of increasing the concentration of the peptide at the membrane, and we conclude that this form of the 27-mer(I860A) provides an outstanding genetically encoded reagent to interdict Gα$_q$-stimulated signaling at the cellular level. It is likely that, although the HTH evolved for optimal physiological activation of PLC-β by Gα$_q$, it did not evolve to provide the highest binding affinity. Indeed, a simple alanine substitution of Ile-860 in PLC-β3 was shown previously empirically to increase Gα$_q$-mediated activation of the lipase, and we show here that such a substitution in HTH also significantly increases HTH binding affinity for Gα$_q$. Thus, both rational and iterative screens of other substitutions in HTH should lead to additional increases in binding affinity in HTH-related peptides, and a long-term goal of this work is to generate Gα$_q$-directed drugs consisting of these peptides packaged in cell-permeable forms. The remarkable capacity of the 27-mer(I860A) in a fluorescent protein-flanked form to block Gα$_q$-stimulated inositol lipid signaling also suggests a starting point to develop, for example, biosensors that image the signaling dynamics of activated Gα$_q$.

Experimental Procedures

Peptides—Peptides were either synthesized in-house using a PS3 solid-state peptide synthesizer (Protein Technologies, Inc.) or by Anaspec. Peptides in-house were purified with a C18 reversed phased HPLC system with a UV detector, and purity was determined to be >95% using analytical reversed phase HPLC. Correct molecular weights of peptides were determined using MALDI-TOF mass spectrometry.

A subset of TAMRA-labeled PLC-β3 peptides following the C2 domain include 9, 12, 25, and 27 residues (9-, 12-, 25-, and 27-mer). An additional TAMRA-27-mer(I860A) contains a point mutation, I860A, as well as a non-natural norleucine (Nle) substituted for methionine at residue 869. All peptides were amidated on the C terminus and acetylated or labeled with TAMRA on the N terminus. Synthesized peptides included different isoforms of PLC-β isozymes and Dbl family GEF proteins shown in Fig. 2*B*. All peptides were dissolved in 10 mM K_2HPO_4 at concentrations of 1–5 mM.

Fluorescence Polarization Assay—Fluorescence polarization assays were performed in small-volume cuvettes (Starna Cells, Inc. Atascadero, CA) in a Fluorolog-3 spectrophotometer (Horiba Scientific, Edison, NJ) that contained a final volume of 60 μl. Fluorescence polarization experiments used 400 nM TAMRA-labeled peptides and monitored the change in polarization at an excitation wavelength of 554 nm and an emission wavelength of 569 nm. Increasing amounts of Gα proteins were added to the TAMRA-labeled peptide solution to determine the affinity of Gα$_q$ for the peptides. Increasing amounts of unlabeled peptides or proteins were added with 400 nM TAMRA-27-mer(I860A) and 800 nM Gα$_q$ to determine the IC$_{50}$ values of the unlabeled peptides. All experiments contained 10 mM HEPES (pH 7.0), 150 mM NaCl, and 50 mM $MgCl_2$ with or without 150 μM $AlCl_3$ plus 50 mM NaF. All K_d and IC$_{50}$ values were calculated using Prism5 using a one-site binding hyperbola ($Y = B_{max} \times X/K_d + X$). For competition experiments, K_i values were calculated from IC$_{50}$ values using an equation derived by Nikolovska-Coleska *et al.* (38).

Protein Expression and Purification—Gα$_q$Δ34, Gα$_q$Δ7, PLC-β3, and PLC-β3(1–886) were purified from High-Five insect cells. Gα$_q$Δ34 was engineered for high level of expression using a chimeric form of Gα$_{q/i}$ that contained an N-terminal hexahistidine tag followed by residues 1–28 of rat Ga$_{i1}$, a tobacco etch virus protease site, and residues 35–359 of mouse Gα$_q$ (Gα$_q$Δ34). Gα$_q$Δ7 was constructed similarly. Purification of Gα$_q$Δ34 and Gα$_q$Δ7 followed protocols published previously (30). PLC-β3 and PLC-β3 (1–886) were purified following protocols published previously (30). The truncated p63RhoGEF pleckstrin homology-Dbl homology (PH-DH) extension (155–493) was purified from *Escherichia coli* and followed protocols published previously (29).

Quantification of Phospholipase Activity of Purified PLC-β3 Isozymes—Basal phospholipase activity was determined by combining 330 μM L-α-phosphatidyl ethanolamine and 30 μM L-α-phosphatidylinositol-4,5-bisphosphate and drying the lipids under N_2 in chloroform solution followed by resuspension by sonication in 20 mM HEPES (pH 7.2). Reactions were incubated for 10 min at 30 °C in a final buffer consisting of 30 mM HEPES (pH 7.2), 70 mM KCl, 2 mM DTT, 16.7 mM NaCl, 3 mM EGTA, 200 nM free Ca^{2+}, 0.17 mg/ml fatty acid-free BSA, 10 mM NaF, 30 μM $AlCl_3$, 2.7 mM $MgCl_2$, and 20,000 dpm [^{3}H]PIP_2 with 200–300 pM of PLC-β3 to maintain the linearity of the enzyme assay. Increasing amount of peptide were added to the solution containing 60–200 nM Gα$_q$ or 20–60 nM Gβ$_1$γ$_2$.

Transfection of HEK293 Cells and Quantification of [^{3}H]-Inositol Phosphate Accumulation—HEK293 cell-based assays measured accumulation of [^{3}H]inositol phosphates. HEK293 cells were maintained in high-glucose DMEM containing 10% fetal bovine serum, 100 units/ml penicillin, and 100 μg/ml streptomycin at 37 °C in an atmosphere of 95% air/5% CO_2. HEK293 cells were transfected with 100 ng of DNA that encoded the 5HT$_{2A}$ receptor in the pcDNA vector and other indicted DNA vectors using FuGENE 6 (Promega, Madison, WI) according to the protocol of the manufacturer. The total amount of transfected DNA was 400 ng and included empty pcDNA vector to maintain equal amounts of DNA per well. Twenty-four hours post-transfection, media were exchanged, and cells were metabolically labeled with 1 μCi of myo-[2-^{3}H(N)]inositol (American Radiolabeled Chemicals, St. Louis, MO) at 37 °C for 24 h. Metabolic labeling proceeded at 37 °C for 1 h in a water bath with 10 mM LiCl to inhibit phosphatases and 2 μM DOI to stimulate the 5HT$_{2A}$ receptor. Incubations were terminated by aspiration of the culture medium and subsequent addition of 50 mM formic acid for 20 min, followed by neutralization with 150 mM NH_4OH. ^{3}H-labeled inositol

phosphates were isolated and quantified using Dowex chromatography.

Guanine Nucleotide Exchange Assays—The guanine nucleotide exchange activity of purified p63RhoGEF pleckstrin homology-Dbl homology extension (155–493) was determined using a kinetic fluorescence-based assay with RhoA that was preloaded with BODIPY FL-conjugated GDP (BODIPY-GDP, Molecular Probes) as described previously (39). Exchange assays were performed using a Fluorolog-3 (Horiba Scientific) with wavelengths at $\lambda_{excitation}$ = 500 nm (slits = 1 nm), $\lambda_{emission}$ = 511 nm (slits = 1 nm) and 1.5-ml quartz cuvettes thermostated at 20 °C while stirring constantly. Reactions were carried out in exchange buffer consisting of 20 mM Tris (pH 7.5), 150 mM NaCl, 10 mM $MgCl_2$, 10 mM NaF, 30 μM $AlCl_3$, and 10 μM GDP. Exchange assays contained BODIPY-GDP-preloaded RhoA (100 nM) equilibrated in exchange buffer at 20 °C, followed by addition of p63RhoGEF (100 nM), $G\alpha_q$ (100 nM), and the indicated amounts of peptides. Nucleotide exchange was monitored in real time for 2 h at 20 °C.

Electrophysiology—C57BL/6J mice were sacrificed via deep isoflurane anesthesia and rapid decapitation, and brain slices containing the prefrontal cortex (PFC) were prepared as described previously (40, 41). Briefly, brains were rapidly removed, and 300-μm slices were cut on a vibratome (Leica Biosystems, Buffalo Grove, IL) in a cold (1–4 °C) sucrose-based external solution. Slices were then immediately placed in normal artificial cerebrospinal fluid (194 mM sucrose, 20 mM NaCl, 4.4 mM KCl, 2 mM $CaCl_2$, 1 mM $MgCl_2$, 1.2 mM NaH_2PO_4, 10 mM glucose, and 26 mM $NaHCO_3$) saturated with 95% O_2/5% CO_2 and maintained at 30 °C and allowed to recover for at least 1 h. Individual slices were then placed in a holding chamber and continuously perfused with normal oxygenated artificial cerebrospinal fluid maintained at 30 °C at a rate of 2 ml/min. Neurons were visualized using infrared video microscopy (Olympus, Center Valley, PA). Recording electrodes (3–6 megohms) were pulled with a Flaming-Brown micropipette puller (Sutter Instruments, Novato, CA) using thin-walled borosilicate glass capillaries. Signals were acquired by a Multiclamp 700 B amplifier (Molecular Devices, Sunnyvale, CA), digitized at 10 kHz, and analyzed using Clampfit 10.2 software (Molecular Devices). Input resistance and access resistance were continuously monitored throughout all experiments, and those in which changes in access resistance exceeded 20% were excluded from all data analyses.

A previous report showed that activation of $G\alpha_q$-coupled muscarinic acetylcholine 1 receptors (M1) in the PFC elicited a robust inward current in the PFC (36). Whole-cell slice electrophysiology was conducted to assess the ability of the $G\alpha_q$ inhibitory peptide to block $G\alpha_q$-mediated M1 receptor signaling in the PFC in a voltage clamp using a potassium gluconate-based intracellular solution (135 mM K^+ gluconate, 5 mM NaCl, 2 mM $MgCl_2$, 10 mM HEPES, 0.6 mM EGTA, 4 mM Na_2ATP, 0.4 mM Na_2GTP (pH 7.3), 285–290 mosmol) containing spermine (0.1 mM) and the inactive or active peptide (10 μM). Cells were held at −70 mV. After achieving a stable 2-min baseline, we assessed the effects of the M1 receptor agonist carbachol (CCh, 10 μM, bath applied for 10 min) on the holding current in the presence of the active or inactive $G\alpha_q$ inhibitory peptide in the recording pipette. To confirm the effect observed with the inactive $G\alpha_q$ inhibitory peptide in the recording pipette was mediated by the M1 receptor, we assessed the ability of CCh to alter the holding current in the presence of the M1 receptor antagonist pirenzepine (2 μM, bath applied for 10 min).

The effects of CCh in the presence of the inactive or active peptide were analyzed by comparing the change in holding current during the final minute of drug application from the final minute of baseline. To eliminate the possibility that observed drug effects were due to cell rundown, the holding current during the final minute of washout was assessed, and any cells that did not recover baseline holding potential were removed from analyses. A maximum of two cells from each animal and one cell per slice were analyzed. *t* tests were used to analyze differences in the magnitude of the CCh response in the presence of the active *versus* inactive peptide as well as to analyze the difference in holding current in the presence of CCh relative to baseline for each peptide. Similar analyses were used to assess the effect of pirenzepine to block this effect.

Author Contributions—T. H. C. designed and conducted the majority of experiments. G. L. W. conducted the vesicle assay experiments (Fig. 3). E. G. L. G. conducted the neuronal depolarization experiments (Fig. 6). K. K. synthesized all peptides for this study and helped with the selection of specific mutations. Manuscript writing and editing were done by T. H. C., T. K. H., B. D. S., T. L. K., and J. S.

Acknowledgments—We acknowledge S. Hicks for help with experiments monitoring HTH peptides. We are thankful to M. Barrett for his assistance with cell and lipid vesicle experiments.

References

1. Wettschureck, N., and Offermanns, S. (2005) Mammalian G proteins and their cell type specific functions. *Physiol. Rev.* **85,** 1159–1204
2. Rozengurt, E. (2007) Mitogenic signaling pathways induced by G protein-coupled receptors. *J. Cell. Physiol.* **213,** 589–602
3. Gainetdinov, R. R., Premont, R. T., Bohn, L. M., Lefkowitz, R. J., and Caron, M. G. (2004) Desensitization of G protein-coupled receptors and neuronal functions. *Annu. Rev. Neurosci.* **27,** 107–144
4. Hubbard, K. B., and Hepler, J. R. (2006) Cell signalling diversity of the $G\alpha_q$ family of heterotrimeric G proteins. *Cell Signal.* **18,** 135–150
5. Wall, M. A., Coleman, D. E., Lee, E., Iñiguez-Lluhi, J. A., Posner, B. A., Gilman, A. G., and Sprang, S. R. (1995) The structure of the G protein heterotrimer $G_i(\alpha_1\beta_1\gamma_2)$. *Cell* **83,** 1047–1058
6. Lambright, D. G., Sondek, J., Bohm, A., Skiba, N. P., Hamm, H. E., and Sigler, P. B. (1996) The 2.0 Å crystal structure of a heterotrimeric G protein. *Nature* **379,** 311–319
7. Adjobo-Hermans, M. J., Goedhart, J., van Weeren, L., Nijmeijer, S., Manders, E. M., Offermanns, S., and Gadella, T. W., Jr. (2011) Real-time visualization of heterotrimeric G protein G_q activation in living cells. *BMC Biol.* **9,** 32
8. Yu, J. Z., and Rasenick, M. M. (2002) Real-time visualization of a fluorescent $G\alpha_s$: dissociation of the activated G protein from plasma membrane. *Mol. Pharmacol.* **61,** 352–359
9. Milligan, G., and Kostenis, E. (2006) Heterotrimeric G-proteins: a short history. *Br. J. Pharmacol.* **147,** S46–55
10. Smrcka, A. V. (2013) Molecular targeting of $G\alpha$ and $G\beta\gamma$ subunits: a potential approach for cancer therapeutics. *Trends Pharmacol. Sci.* **34,** 290–298
11. Prévost, G. P., Lonchampt, M. O., Holbeck, S., Attoub, S., Zaharevitz, D., Alley, M., Wright, J., Brezak, M. C., Coulomb, H., Savola, A., Huchet, M., Chaumeron, S., Nguyen, Q. D., Forgez, P., Bruyneel, E., *et al.* (2006) Anti-

cancer activity of BIM-46174, a new inhibitor of the heterotrimeric Gα/Gβγ protein complex. *Cancer Res.* **66,** 9227–9234
12. Ayoub, M. A., Damian, M., Gespach, C., Ferrandis, E., Lavergne, O., De Wever, O., Banères, J. L., Pin, J. P., and Prévost, G. P. (2009) Inhibition of heterotrimeric G protein signaling by a small molecule acting on Gα subunit. *J. Biol. Chem.* **284,** 29136–29145
13. Schmitz, A. L., Schrage, R., Gaffal, E., Charpentier, T. H., Wiest, J., Hiltensperger, G., Morschel, J., Hennen, S., Häußler, D., Horn, V., Wenzel, D., Grundmann, M., Büllesbach, K. M., Schröder, R., Brewitz, H. H., *et al.* (2014) A cell-permeable inhibitor to trap Gα proteins in the empty pocket conformation. *Chem. Biol.* **21,** 890–902
14. Taniguchi, M., Nagai, K., Arao, N., Kawasaki, T., Saito, T., Moritani, Y., Takasaki, J., Hayashi, K., Fujita, S., Suzuki, K., and Tsukamoto, S. (2003) YM-254890, a novel platelet aggregation inhibitor produced by *Chromobacterium* sp. QS3666. *J. Antibiot.* **56,** 358–363
15. Zaima, K., Deguchi, J., Matsuno, Y., Kaneda, T., Hirasawa, Y., and Morita, H. (2013) Vasorelaxant effect of FR900359 from *Ardisia crenata* on rat aortic artery. *J. Nat. Med.* **67,** 196–201
16. Miyamae, A., Fujioka, M., Koda, S., and Morimoto, Y. (1989) Structural studies of FR900359, a novel cyclic desipeptide from *Ardisia crenata* Sims (Myrsinaceae). *J. Chem. Soc. Perkin Trans.* 873–878
17. Taniguchi, M., Suzumura, K., Nagai, K., Kawasaki, T., Takasaki, J., Sekiguchi, M., Moritani, Y., Saito, T., Hayashi, K., Fujita, S., Tsukamoto, S., and Suzuki, K. (2004) YM-254890 analogues, novel cyclic depsipeptides with Gα$_{q/11}$ inhibitory activity from *Chromobacterium* sp. QS3666. *Bioorg. Med. Chem.* **12,** 3125–3133
18. Takasaki, J., Saito, T., Taniguchi, M., Kawasaki, T., Moritani, Y., Hayashi, K., and Kobori, M. (2004) A novel Gα$_{q/11}$-selective inhibitor. *J. Biol. Chem.* **279,** 47438–47445
19. Nishimura, A., Kitano, K., Takasaki, J., Taniguchi, M., Mizuno, N., Tago, K., Hakoshima, T., and Itoh, H. (2010) Structural basis for the specific inhibition of heterotrimeric G$_q$ protein by a small molecule. *Proc. Natl. Acad. Sci. U.S.A.* **107,** 13666–13671
20. Johnston, C. A., Willard, F. S., Ramer, J. K., Blaesius, R., Roques, C. N., and Siderovski, D. P. (2008) State-selective binding peptides for heterotrimeric G-protein subunits: novel tools for investigating G-protein signaling dynamics. *Comb. Chem. High Throughput Screen.* **11,** 370–381
21. Kimple, R. J., De Vries, L., Tronchère, H., Behe, C. I., Morris, R. A., Gist Farquhar, M., and Siderovski, D. P. (2001) RGS12 and RGS14 GoLoco motifs are Gα$_i$ interaction sites with guanine nucleotide dissociation inhibitor activity. *J. Biol. Chem.* **276,** 29275–29281
22. Webb, C. K., McCudden, C. R., Willard, F. S., Kimple, R. J., Siderovski, D. P., and Oxford, G. S. (2005) D2 dopamine receptor activation of potassium channels is selectively decoupled by Gα-specific GoLoco motif peptides. *J. Neurochem.* **92,** 1408–1418
23. Johnston, C. A., Ramer, J. K., Blaesius, R., Fredericks, Z., Watts, V. J., and Siderovski, D. P. (2005) A bifunctional Gα$_i$/Gα$_s$ modulatory peptide that attenuates adenylyl cyclase activity. *FEBS Lett.* **579,** 5746–5750
24. Johnston, C. A., Lobanova, E. S., Shavkunov, A. S., Low, J., Ramer, J. K., Blaesius, R., Fredericks, Z., Willard, F. S., Kuhlman, B., Arshavsky, V. Y., and Siderovski, D. P. (2006) Minimal determinants for binding activated Gα from the structure of a Gα$_{i1}$-peptide dimer. *Biochemistry* **45,** 11390–11400
25. Johnston, C. A., Willard, F. S., Jezyk, M. R., Fredericks, Z., Bodor, E. T., Jones, M. B., Blaesius, R., Watts, V. J., Harden, T. K., Sondek, J., Ramer, J. K., and Siderovski, D. P. (2005) Structure of Gα$_{i1}$ bound to a GDP-selective peptide provides insight into guanine nucleotide exchange. *Structure* **13,** 1069–1080
26. Sprang, S. R. (1997) G protein mechanisms: insights from structural analysis. *Annu. Rev. Biochem.* **66,** 639–678
27. Harden, T. K., Waldo, G. L., Hicks, S. N., and Sondek, J. (2011) Mechanism of activation and inactivation of G$_q$/phospholipase C-β signaling nodes. *Chem. Rev.* **111,** 6120–6129
28. Aittaleb, M., Boguth, C. A., and Tesmer, J. J. (2010) Structure and function of heterotrimeric G protein-regulated Rho guanine nucleotide exchange factors. *Mol. Pharmacol.* **77,** 111–125
29. Rojas, R. J., Yohe, M. E., Gershburg, S., Kawano, T., Kozasa, T., and Sondek, J. (2007) Gα$_q$ directly activates p63RhoGEF and Trio via a conserved extension of the Dbl homology-associated pleckstrin homology domain. *J. Biol. Chem.* **282,** 29201–29210
30. Waldo, G. L., Ricks, T. K., Hicks, S. N., Cheever, M. L., Kawano, T., Tsuboi, K., Wang, X., Montell, C., Kozasa, T., Sondek, J., and Harden, T. K. (2010) Kinetic scaffolding mediated by a phospholipase C-β and G$_q$ signaling complex. *Science* **330,** 974–980
31. Lutz, S., Shankaranarayanan, A., Coco, C., Ridilla, M., Nance, M. R., Vettel, C., Baltus, D., Evelyn, C. R., Neubig, R. R., Wieland, T., and Tesmer, J. J. (2007) Structure of Gα$_q$-p63RhoGEF-RhoA complex reveals a pathway for the activation of RhoA by GPCRs. *Science* **318,** 1923–1927
32. Jhon, D. Y., Lee, H. H., Park, D., Lee, C. W., Lee, K. H., Yoo, O. J., and Rhee, S. G. (1993) Cloning, sequencing, purification, and G$_q$-dependent activation of phospholipase C-β3. *J. Biol. Chem.* **268,** 6654–6661
33. Smrcka, A. V., and Sternweis, P. C. (1993) Regulation of purified subtypes of phosphatidylinositol-specific phospholipase C-β by G protein α and βγ subunits. *J. Biol. Chem.* **268,** 9667–9674
34. Lyon, A. M., Dutta, S., Boguth, C. A., Skiniotis, G., and Tesmer, J. J. (2013) Full-length Gα$_q$-phospholipase C-β3 structure reveals interfaces of the C-terminal coiled-coil domain. *Nat. Struct. Mol. Biol.* **20,** 355–362
35. Lyon, A. M., Tesmer, V. M., Dhamsania, V. D., Thal, D. M., Gutierrez, J., Chowdhury, S., Suddala, K. C., Northup, J. K., and Tesmer, J. J. (2011) An autoinhibitory helix in the C-terminal region of phospholipase C-β mediates Gα$_q$ activation. *Nat. Struct. Mol. Biol.* **18,** 999–1005
36. Carr, D. B., and Surmeier, D. J. (2007) M1 muscarinic receptor modulation of Kir2 channels enhances temporal summation of excitatory synaptic potentials in prefrontal cortex pyramidal neurons. *J. Neurophysiol.* **97,** 3432–3438
37. Shankaranarayanan, A., Boguth, C. A., Lutz, S., Vettel, C., Uhlemann, F., Aittaleb, M., Wieland, T., and Tesmer, J. J. (2010) Gα$_q$ allosterically activates and relieves autoinhibition of p63RhoGEF. *Cell Signal.* **22,** 1114–1123
38. Nikolovska-Coleska, Z., Wang, R., Fang, X., Pan, H., Tomita, Y., Li, P., Roller, P. P., Krajewski, K., Saito, N. G., Stuckey, J. A., and Wang, S. (2004) Development and optimization of a binding assay for the XIAP BIR3 domain using fluorescence polarization. *Anal. Biochem.* **332,** 261–273
39. Rojas, R. J., Kimple, R. J., Rossman, K. L., Siderovski, D. P., and Sondek, J. (2003) Established and emerging fluorescence-based assays for G-protein function: Ras-superfamily GTPases. *Comb. Chem. High Throughput Screen.* **6,** 409–418
40. Mozhui, K., Karlsson, R. M., Kash, T. L., Ihne, J., Norcross, M., Patel, S., Farrell, M. R., Hill, E. E., Graybeal, C., Martin, K. P., Camp, M., Fitzgerald, P. J., Ciobanu, D. C., Sprengel, R., Mishina, M., *et al.* (2010) Strain differences in stress responsivity are associated with divergent amygdala gene expression and glutamate-mediated neuronal excitability. *J. Neurosci.* **30,** 5357–5367
41. Li, C., Pleil, K. E., Stamatakis, A. M., Busan, S., Vong, L., Lowell, B. B., Stuber, G. D., and Kash, T. L. (2012) Presynaptic inhibition of γ-aminobutyric acid release in the bed nucleus of the stria terminalis by κ opioid receptor signaling. *Biol. Psychiatry* **71,** 725–732